

Tonotopic Sensitivity to Supra-threshold Hearing Deficits of the Envelope Following Response Evoked by Broadband Stimuli

Sarineh KESHISHZADEH¹; Viacheslav VASILKOV²; Sarah VERHULST³

Hearing Technology @WAVES, Dept. of Information Technology, Ghent University, Belgium

ABSTRACT

Scalp-recorded electrophysiological Envelope Following Responses (EFRs) have recently gained popularity as an objective measure of supra-threshold hearing deficits (e.g., as caused by cochlear synaptopathy). To explore the frequency specificity of EFRs in diagnosing deficits, we recorded EFRs to sinusoidally amplitude-modulated (AM) white noise carriers with different bandwidths in two participant groups: young normal-hearing control group and a group self-reported hearing difficulties in noisy listening environments. Despite individual variability in EFR strength, the group-means revealed minor response differences in stimuli with different low-frequency content. The limited contribution of auditory frequency channels below 2 kHz to the EFR was confirmed through EFR simulations from a biophysically-inspired model of the human auditory periphery. Further investigation showed that the minor low-frequency contribution stems from the lack of AM coding in individual low-frequency channels, although the overall spike-rate increases for stimulation with wider carrier bands. In conclusion, despite the broadband cochlear excitation, the broadband EFR mostly reflects summed AM coding strength in frequency channels above 2 kHz. To increase the frequency sensitivity of the EFRs it is necessary to carefully investigate the bandwidth and modulation frequency of the stimulus.

Keywords: Envelope Following Responses, Frequency sensitivity, Broadband modulated stimuli

1. INTRODUCTION

Threshold audiometry at frequencies between 250-8000Hz does not quantify the possible supra-threshold hearing deficits in listeners with normal hearing thresholds. One of the possible sources of supra-threshold hearing deficits is loss of auditory nerve (AN) fibers (i.e., cochlear synaptopathy) as a result of noise exposure or aging. The synaptopathy leaves the outer-hair-cells intact and does not affect the audiometric thresholds. Recently, auditory evoked potentials such as Auditory Brainstem Responses (ABRs) and Envelope Following Responses (EFRs) have been proposed to quantify these supra-threshold hearing deficits. EFRs reflect the phase-locking strength to the modulated sounds (1) and are sensitive to synaptopathy in animals (2). Hence, EFRs could be more robust metric to measure these types of fibers synchrony to the modulated stimulus. However, EFRs are confounded by stimulus and subject-specific factors (3, 4) as well as the spread of the basilar-membrane excitation (5).

To evaluate the diagnostic power and tonotopy of frequency-specific EFRs in humans, we investigated which cochlear frequency regions contribute to the scalp-recorded population response. Therefore, we took an experimental approach in which we adopted, (i) white-noise carriers of various bandwidths with different low cut-off frequencies, (ii) stimuli with a modulation frequency (MF) of 120 Hz to avoid cortical contributions to the response and (iii) a stimulus level of 70-dB-SPL to encompass the contribution of a range of low and high-threshold AN fibers to the EFR. We recorded EFRs in groups with normal audiograms but with or without self-reported hearing difficulties in noisy environments. The former group might be representative of the target synaptopathy expected group without hearing thresholds deficits.

To further investigate the origin of the experimental EFRs differences to noise carriers of different bandwidths, we adopted a model-based approach (6). The model offers a promising way to further explore the influence of different stimuli characteristics on the frequency sensitivity along the

¹ Sarineh.Keshishzadeh@ugent.be

² Viacheslav.Vasilkov@ugent.be

³ S.Verhulst@ugent.be

different processing levels of the auditory periphery (i.e., cochlea, AN and brainstem). Given that previous studies have shown that increasing the MF of a broadband noise, increases the behavioral AM detection thresholds (7) and decreases the EFR amplitudes (8), we focused on investigating the effect of different modulation frequencies in encoding the stimulus envelope in basilar membrane (BM) velocity and AN spike rates.

First, the experimental stimuli and the participated groups are described. After which Sections 2 and 3 detail the implemented methods and show comparisons between experimental and simulated EFRs. Finally, the discussion states possible reasons for the lack of AM coding in the experimental data at lower frequencies and make suggestions to improve the broadband EFRs frequency sensitivity based on the model simulations.

2. Methods

EFRs were recorded to five filtered white-noise carriers in [0.25-22], [0.5-22], [1-22], [2-22] and [4-22] kHz frequency bands and were 100% modulated with a 120 Hz pure tone. The spectrally widest stimulus was presented at 70-dB-SPL and the other bandwidth stimuli had lower level to maintain a similar spectral level in all filtered stimuli. The stimulus epochs were 1.25-s long and repeated 370 times. EFRs were recorded with a 64-channel Biosemi EEG system. Details of the experimental setup were described elsewhere (9). Sixteen normal-hearing (NH) subjects aged 18-30 years (24.21±4.10 years, six female) and nine audiometric normal hearing subjects with self-reported hearing difficulties in noisy environments (NHSR) aged 23-49 (33.78±8.57 years, three female) participated in the experiment. All participants had hearing thresholds below 25 dB-HL, except for one participant who had 30 dB-HL loss at 250 Hz. The best audiometric ear at 4 kHz was chosen for the monaural stimulation. During the recording, the subjects were seated in a comfortable chair in an acoustically and electrically shielded sound booth watching silent movies with subtitles to keep them awake. All participants were informed about the experimental procedure according to the ethical procedure at Ghent University and an informed consent was received.

2.1 Experimental Data Analysis

For each condition, the responses from the Cz channel were filtered between 60 and 600 Hz with a 800th order Blackman window-based band-pass FIR filter in MATLAB using the `filtfilt` function. Then, the signals were epoched in 1-s long blocks starting 0.25 after the stimulus onset to focus on the steady state part of the response. A baseline correction was applied by subtracting the average of each epoch, before averaging across trials. Thirty epochs with the highest peak-to-trough absolute values were removed to drop noisiest epochs and keep an equal number of epochs to average for all conditions and subjects. We adopted a bootstrapping method to identify the EFR strength and signal-to-noise ratio in the frequency domain (10): First, the Fast Fourier Transform (FFT) of each epoch was computed. Then, an averaged FFT over 340 epochs randomly drawn with replacement out of total epochs was calculated. This procedure was repeated 200 times and resulted in a nearly Gaussian distribution of mean spectra of the responses. The absolute value of the mean of 200 averaged epochs, yielded the EFRs in the frequency domain. Secondly, the same procedure was followed with 1000 (of which half were phase-flipped) repeated averages to estimate the noise-floor. Finally, the subtraction between the absolute values of the signal and noise-floor averages resulted in the stimulus-driven EFR spectrum. To calculate the EFR strength, we included the magnitude of fundamental MF and any visible harmonics. Only two harmonics were visible in our data, we hence considered the magnitude of the fundamental frequency of the modulator (i.e., $f_0=120$ Hz) and two harmonics:

$$EFR_{strength} = \sum_{i=0}^2 |Magnitude_{f_i}| \quad (1)$$

2.2 Modelling Approach

We simulated EFRs using a biophysically-inspired model of the human auditory periphery (6). The same stimuli as were adopted in the experiment presented to the model, but with a total duration of 600 ms. The last 400 ms of the simulated responses were used for the EFR calculation. Further analysis steps were identical to the experimental data analysis. Given that the stimulus was noise, simulated responses were averaged 100 times before calculating the EFR. The modelling approach, brings the benefit of allowing a frequency-specific investigation of the sources contributing to the EFRs to

modulated broadband stimuli at both the BM and AN processing levels. To this end, we explored the energy, i.e., the root-mean-square (RMS), and modulation strength at each simulated characteristic frequency (CF) channel. We calculated the modulation strength at both BM and AN levels in the time domain by averaging the BM velocity and AN spike rates across all cycles for each epoch. For a MF of 120 Hz, each epoch encompasses 48 cycles and taking into account the 100 repetitions of the stimulus representation, the half of the peak-to-peak amplitude of the 4800 averages were defined as the modulation strength of each CF channel. We followed the same procedure to calculate the modulation strength for the AN simulations to keep a fair comparison with the BM simulations.

3. Results

3.1 EFR Magnitudes Evoked by Broadband Stimuli

Figure 1, shows the EFR magnitudes for the different stimulus conditions and groups (i.e., NH and NHSR). Even though the data points for each condition show individual variabilities, the group-means were constant across conditions for stimuli of low cut-off frequencies up to 2 kHz. A decrement was observed for the last condition with the stimulus bandwidth of [4-22] kHz. The normal-hearing model-predicted EFRs (diamonds in Figure 1), reveals the same trend as the experimental group-means across conditions. The NHSR group-mean EFRs of the participants were lower than the EFRs of the NH participants in each condition. This finding is consistent with the idea that NHSR listeners may suffer from supra-threshold hearing deficits.

3.2 CF Contributions to the EFR

To explore the origin of the frequency-dependent behavior of the EFRs, we studied the contribution of different CF channels for different stimulus conditions to population responses at BM and AN levels of the model. Figure 2 shows simulated excitation patterns and modulation responses to the experimental stimuli of BM velocity (Figure 2a and 2b) and AN responses (Figure 2c and 2d). The excitation pattern shows increased velocity at CF channels corresponding to those contained in the stimulus frequency, while the BM modulation response, shows a sloping response starting one octave below the excited CF channels, and a constant behavior at CF channels above the 4 kHz. A similar pattern can be observed at the AN level, where a sharp increase in spike rate is observed for frequencies contained in the stimulus in the excitation pattern. A sloping spike rate increment in modulation response was again observed when evaluating the modulated response at AN. Since the EFR is a population response across the CF channels, the overlapping modulation response for the first three conditions, explain the equal group-means observed in the experimental data in Figure 1.

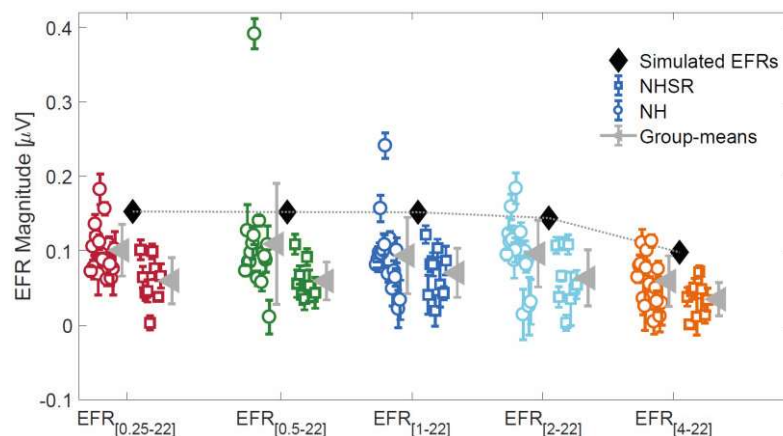


Figure 1 – Recorded EFR magnitudes in NH (circles) and NHSR (squares) listeners. The corresponding group-means are shown with left pointing triangles. Simulated EFRs for a normal-hearing model are shown by black diamonds.

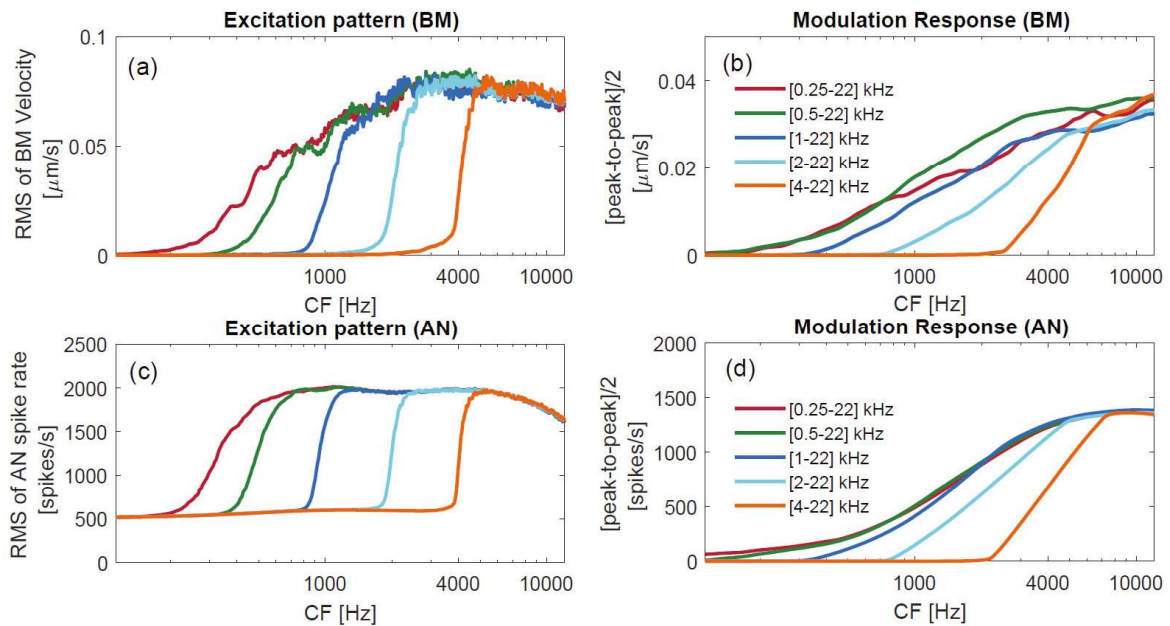


Figure 2 – Simulated excitation patterns and modulation responses calculated for each CF channel to the experimental stimuli from the BM (a and b) and AN (c and d) processing levels of the model.

To investigate the absence of AM coding at low CFs for 120 Hz modulator, we further evaluated the effect of MF and CF contributions to the modulated response in the broadest bandwidth condition, i.e., [0.25-22] kHz. First, a time domain visualization from two CF channels is shown in Figure 3, for MFs of 20 and 120 Hz. CF channels of 500 and 4000 Hz are shown and evaluated for their AM content at the BM velocity (Figure 3a) and AN spike rate (Figure 3b). Both responses to non-modulated and modulated broadband stimuli are shown and the response from CF=500 Hz shows no noticeable difference between non-modulated and 120 Hz modulated noise at both BM and AN processing levels. However at the CF=4000Hz the effect of MF can be observed. A more direct comparison of the modulation strength at two CF channels was made in Figures 3c and d at BM and AN levels, where the 4800 averaged cycles at 120 Hz MF and $8 \times 100 = 800$ averaged cycles at 20 Hz MF are shown. These figures reveal the lack of modulation response at 120 Hz MF in low CF channel (500 Hz) at both BM and AN levels, which are in agreement with Figure 2b and c, where no modulation response can be seen at low CFs.

4. Discussion

The simulation results in response to broadband stimuli confirmed that there is a reduced contribution from lower CF channels and higher modulation frequencies (120 Hz) at the AN level to the EFR. To study the impact of MF and different cochlea CF regions sensitivity to the EFR, Figure 4 compares the excitation pattern and modulation response of BM velocity and AN spike rates in response to a range of modulation frequencies between 20 and 120 Hz. Although there is an approximately equal excitation pattern in all MFs at both BM and AN levels (Figure 4a and c), the modulation responses show different behavior for different MFs. For a specific MF, the modulation response at BM and AN increases from the apical end to the base. Decreasing the MF, enhances the modulation response at all CFs, especially at the basal end and at the BM level (Figure 4b). Even though the AN level largely reflects the response from the cochlea, we observe that the sloping and increasing modulation response saturates for higher CFs to a fixed MF. Therefore, in spite of an increased modulation response at BM level with decreasing MF, especially at higher CFs, the saturation mechanism at the AN level (due to saturating AN fibers) moves the EFR frequency sensitivity to the lower CFs. One of the possible reasons for the enhanced modulated response of lower MFs at BM, could be the wider filters at higher CFs where more sidebands of the noise-carrier fall inside the cochlear filters and increase the energy of the modulation response. In this context, increasing the MF moves the sidebands further away from the carrier component and decreases the modulation response within a single CF channel (11).

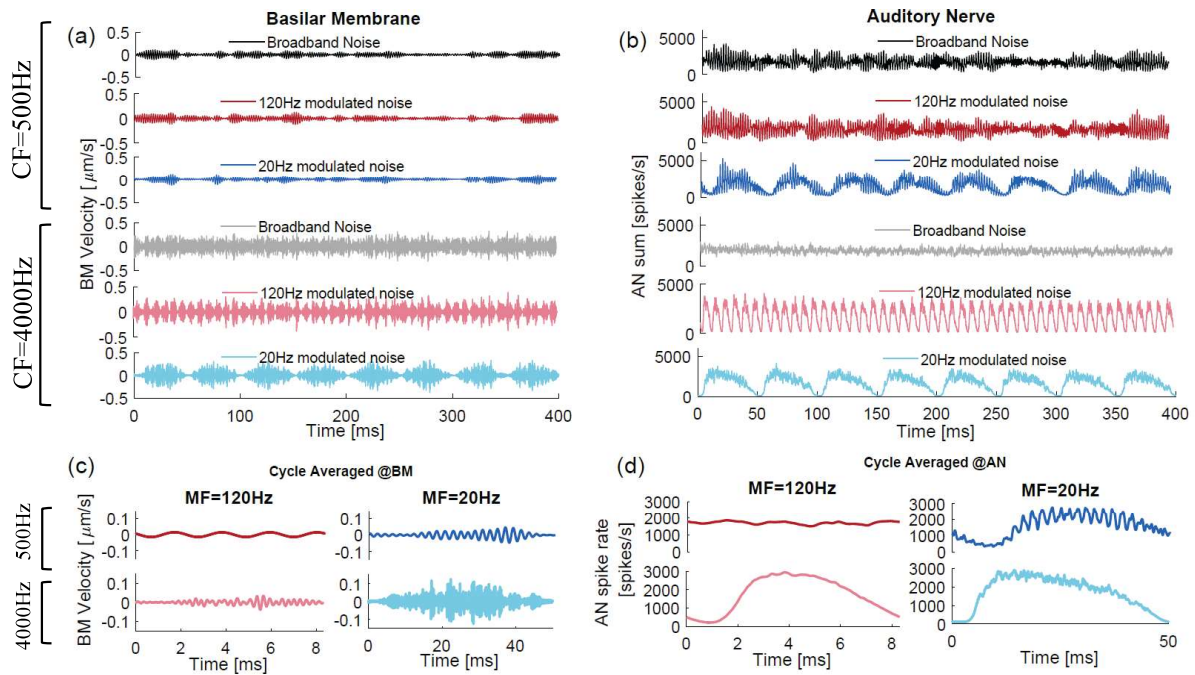


Figure 3—One hundred averaged simulated time-domain epochs in response to broadband stimuli modulated with different MFs in two CF channels at the (a) BM and (b) AN levels of the model. The averaged cycles across each epoch at (c) BM and (d) AN levels.

Based on the model simulations, we conclude that the equal magnitude EFRs for the first three experimental conditions is a consequence of small differences of the curve area of under MF=120 Hz AN modulation response at low CFs and the saturation which occurs at about 4 kHz and higher CFs (Figure 4d). The decrement in the EFR for [4-22] kHz experimental condition is caused by the larger difference between areas under the curves with the previous, broader conditions (shown with dashed lines in Figure 4b and d). The model study suggests that for broadband noise stimuli, modulation frequencies lower than 120 Hz can provide a better tonotopic-sensitive EFRs for lower CFs. However, there is a possibility of contribution from higher auditory processing levels to be involved in the response.

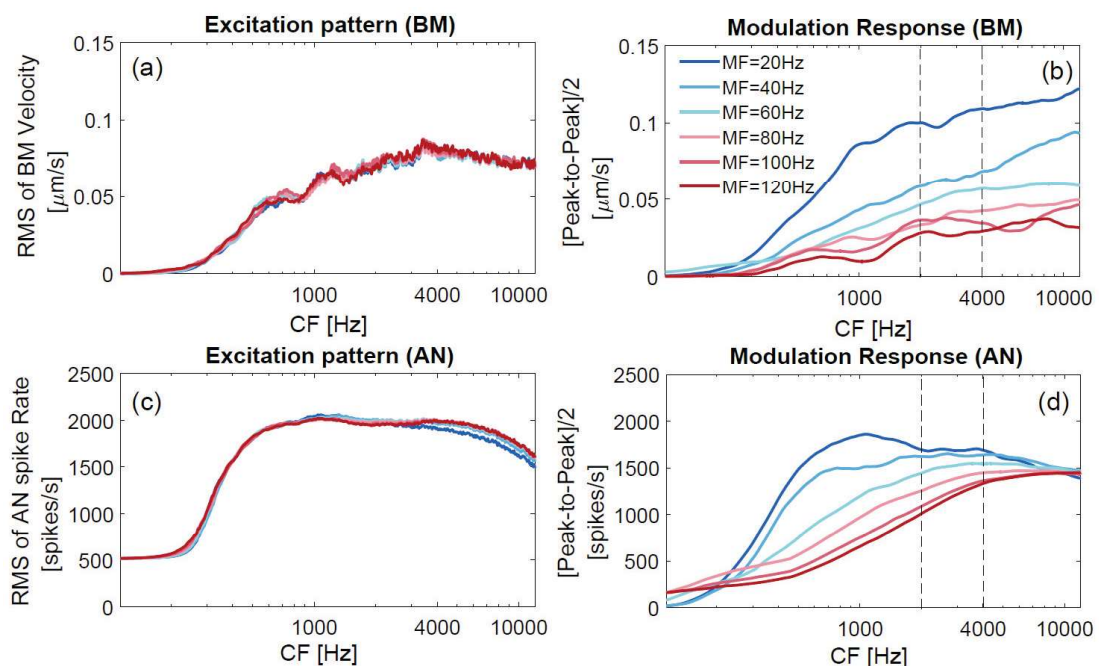


Figure 4—Excitation patterns and modulation responses at BM (a and b) and AN (c and d) levels for different MFs.

ACKNOWLEDGEMENTS

Work supported by European Research Council starting grant ERC-StG-678120 (RobSpear).

REFERENCES

1. Shaheen LA, Valero MD, Liberman MC. Towards a diagnosis of cochlear neuropathy with envelope following responses. *Journal of the Association for Research in Otolaryngology*. 2015;16(6):727-45.
2. Parthasarathy A, Kujawa SG. Synaptopathy in the aging cochlea: Characterizing early-neural deficits in auditory temporal envelope processing. *Journal of Neuroscience*. 2018;38(32):7108-19.
3. Trune DR, Mitchell C, Phillips DS. The relative importance of head size, gender and age on the auditory brainstem response. *Hearing research*. 1988;32(2-3):165-74.
4. Mitchell C, Phillips DS, Trune DR. Variables affecting the auditory brainstem response: audiogram, age, gender and head size. *Hearing research*. 1989;40(1-2):75-85.
5. Bharadwaj HM, Masud S, Mehraei G, Verhulst S, Shinn-Cunningham BG. Individual differences reveal correlates of hidden hearing deficits. *Journal of Neuroscience*. 2015;35(5):2161-72.
6. Verhulst S, Altoe A, Vasilkov V. Computational modeling of the human auditory periphery: Auditory-nerve responses, evoked potentials and hearing loss. *Hearing research*. 2018;360:55-75.
7. Kohlrausch A, Fassel R, Dau T. The influence of carrier level and frequency on modulation and beat-detection thresholds for sinusoidal carriers. *The Journal of the Acoustical Society of America*. 2000;108(2):723-34.
8. Purcell DW, John SM, Schneider BA, Picton TW. Human temporal auditory acuity as assessed by envelope following responses. *The Journal of the Acoustical Society of America*. 2004;116(6):3581-93.
9. Garrett M, Verhulst S. Applicability of subcortical EEG metrics of synaptopathy to older listeners with impaired audiograms. *bioRxiv*. 2018:479246.
10. Zhu L, Bharadwaj H, Xia J, Shinn-Cunningham B. A comparison of spectral magnitude and phase-locking value analyses of the frequency-following response to complex tones. *The Journal of the Acoustical Society of America*. 2013;134(1):384-95.
11. Joris P, Schreiner C, Rees A. Neural processing of amplitude-modulated sounds. *Physiological reviews*. 2004;84(2):541-77.

Proceedings of the

ICA 2019 AND EAA EUROREGIO

23rd International Congress on Acoustics,
integrating 4th EAA Euroregio 2019

9 - 13 September 2019, Aachen, Germany



ISSN 2226-7808 and 2415-1599
ISBN 978-3-939296-15-7